THE JOURNAL OF BIOLOGICAL CHEMISTRY VOL. 291, NO. 44, pp. 23101–23111, October 28, 2016

The Rab3A-22A Chimera Prevents Sperm Exocytosis by Stabilizing Open Fusion Pores*

Received for publication, March 31, 2016, and in revised form, August 26, 2016 Published, JBC Papers in Press, September 9, 2016, DOI 10.1074/jbc.M116.729954

María F. Quevedo[1], Ornella Lucchesi[1], Matías A. Bustos[2], Cristian A. Pocognoni, Paola X. De la Iglesia[3], and Claudia N. Tomes[4]

From the IHEM, Universidad Nacional de Cuyo, CONICET, Facultad de Ciencias Médicas, CC56. 5500 Mendoza, Argentina

At the final stage of exocytotis, a fusion pore opens between the plasma and a secretory vesicle membranes; typically, when the pore dilates the vesicle releases its cargo. Sperm contain a large dense-core secretory granule (the acrosome) whose contents are secreted by regulated exocytosis at fertilization. Minutes after the arrival of the triggering signal, the acrosomal and plasma membranes dock at multiple sites and fusion pores open at the contact points. It is believed that immediately afterward, fusion pores dilate spontaneously. Rab3A is an essential component of human sperm exocytotic machinery. Yet, recombinant, persistently active Rab3A halts calcium-triggered secretion when introduced after docking into streptolysin O-permeabilized cells; so does a Rab3A-22A chimera. Here, we applied functional assays, electron and confocal microscopy to show that the secretion blockage is due to the stabilization of open fusion pores. Other novel findings are that sperm SNAREs engage in α-SNAP/NSF-sensitive complexes at a post-fusion stage. Complexes are disentangled by these chaperons to achieve vesiculation and acrosomal contents release. Thus, post-fusion regulation of the pores determines their expansion and the success of the acrosome reaction.

Exocytosis is a fundamental process used by eukaryotic cells to release biological compounds and to insert lipids and proteins in the plasma membrane. To release all or part of their contents to the extracellular space, secretory vesicles must be transported to the cell periphery, dock to the plasma membrane, and undergo a priming reaction that enables them to fuse upon calcium elevation (1, 2). During fusion with the plasma membrane, the vesicle lumen is initially connected to the extracellular space via a narrow fusion pore through which vesicular contents might be secreted (1, 3–5). Fusion generates an Ω-shaped membrane profile. It was believed that the pore either dilated (full collapse) or resealed (kiss and run), but the existence of a larger spectrum of membrane fates has been recently unveiled (6, 7).

Sperm contain a single, large, dense-core secretory granule (the acrosome); its contents are secreted by regulated exocytosis (acrosome reaction, AR)[5] in the female tract at fertilization or in the test tube in response to calcium (8, 9). Minutes after the arrival of the triggering signal, the acrosomal matrix swells, the granule releases calcium into the cytoplasm and the outer acrosomal membrane forms inward invaginations, whose protruding edges dock (contacts shorter than 8 nm) to the plasma membrane (10, 11). Fusion pores open at the contact points, connecting the outer acrosomal membrane and the overlying plasma membrane. Ω-shaped structures are not observed because the acrosome is as large as the area of plasma membrane it is fusing with. Neither full collapse nor kiss and run exocytosis happen during the AR. Instead, joining of pores generates hybrid plasma-outer acrosomal membrane vesicles, which shed, together with parts of the cytosol and the acrosomal contents, to complete exocytosis (reviewed in Refs. 12, 13). Despite lack of direct evidence, it is presumed that fusion pores dilate spontaneously, immediately after opening.

During membrane fusion, Rab proteins direct the recognition and physical attachments of the compartments that are going to fuse (14–16). Rabs3 and 27 are members of the Rab subfamilies implicated in regulated exocytosis. These "secretory Rabs" localize to vesicles and secretory granules in a variety of secretory cell types (17–21). Rab3 is probably the most studied Rab in exocytotic cells, and the most controversial. Different approaches show both positive and negative roles for various members of the Rab3 family. Sperm Rab3A is activated (exchanges GDP for GTP) in the acrosomal region of human sperm in response to exocytosis inducers (22–25). Later on, Rab3 must be inactivated (hydrolyze GTP) to accomplish vesiculation of the acrosomal and plasma membranes (26). Recombinant, persistently active Rab3A is a molecule with dual properties evidenced at different times and within different molecular contexts during the secretory cascade. Rab3A's positive function is

* This study was supported by Agencia Nacional de Promoción Científica y Tecnológica (Grant numbers PICT2010-0342 and PICT2013-1216, Argentina) and Secretaría de Ciencia y Técnica-Universidad Nacional de Cuyo (Grant number 06/J416, Argentina) (to C. N. T.). The authors declare that they have no conflicts of interest with the contents of this article.

[1] Both authors contributed equally to this work.
[2] Present address: Dept. of Molecular Oncology, John Wayne Cancer Institute, Santa Monica, CA 90404.
[3] Present address: Servicio de Patología, Hospital Italiano de Buenos Aires C1199ABD, Buenos Aires, Argentina.
[4] To whom correspondence should be addressed. E-mail: ctomes@fcm.uncu.edu.ar.

[5] The abbreviations used are: AR, acrosome reaction; 2-APB, 2-aminoethoxydiphenyl borate; BAPTA-AM, (1,2-bis(o-aminophenoxy)ethane-*N*,*N*,*N*′,*N*′-tetraacetic acid)-acetoxymethyl ester; BoNT/B, botulinum neurotoxin B; FITC, fluorescein isothiocyanate; Fuo3-AM, 1-[2-amino-5-(2,7-dichloro-6-hydroxy-3-oxo-9-xanthenyl) phenoxy]-2-(2-amino-5-methylphenoxy)-ethane-*N*,*N*,*N*′,*N*′-tetraacetic acid, pentaacetoxymethyl ester; GTP-γ-S, guanosine 5′-O-triphosphate; IP_3, inositol 1,4,5-trisphosphate; NP-EGTA-AM, *O*-nitrophenyl EGTA-acetoxymethyl ester; NSF, *N*-ethylmaleimide-sensitive factor; PSA, *Pisum sativum* agglutinin; SLO, streptolysin O; α-SNAP, α-soluble NSF-attachment protein; TPEN, *N*,*N*,*N*′,*N*′-tetrakis (2-pyridymethyl) ethylenediamine; TRITC, tetramethyl-rhodamine isothiocyanate.

evidenced when introduced into SLO-permeabilized cells at the beginning of the incubation: the protein triggers exocytosis. Its negative role is manifested when added after docking of the acrosome to the plasma membrane: Rab3A blocks the AR (26). The different effects of recombinant Rab3A in the AR correlate with the activation and inactivation of endogenous Rab3. The positive and negative attributes of recombinant Rab3A are segregated to different domains of the protein. A chimeric protein consisting of the amino-terminal portion of Rab3A fused to the carboxyl-terminal portion of Rab22A bears the repressing capacity of Rab3A. Recombinant, full-length Rab22A has no measurable influence on the calcium-triggered AR, which suggests that the effects elicited by the chimera are attributable to the Rab3A portion of the molecule (26). We employ here this newly developed tool to explore the inhibitory mechanism of Rab3A in the AR. Rab3A-22A halts exocytosis after swelling, intra-acrosomal calcium mobilization and the opening of fusion pores but prior to the vesiculation of membranes and release of acrosomal contents. In other words, Rab3A-22A stabilizes fusion pores and prevents their expansion.

Results and Discussion

Rab3A-22A Prevents Shedding of the Compartment that Contains Endogenous Rab3—The acrosomal region of the sperm head contains the acrosomal granule plus the portions of cytosol and plasma membrane that overlie it. Endogenous Rab3 is detected in the acrosomal region in human sperm by indirect immunofluorescence (26, 27). Because the head is so small, more refined localization analyses within this region, such as whether the protein is soluble or bound to membranes, and if so, to which membranes, are not appreciated by conventional fluorescence microscopy. We investigated whether delivery of the chimera into sperm affected the compartment that contains endogenous Rab3. Sperm untreated (control), incubated with calcium alone (calcium), or incubated with the chimera followed by calcium (Rab3A-22A→calcium) were tripled stained for Rab3 (indirect immunofluorescence with anti-Rab3 antibodies, red), presence of the acrosome (FITC-PSA, green), and nucleus (Hoechst 33342, blue). In unreacted cells, the acrosomes were stained green by FITC-PSA (Fig. 1, cells a′, b′, d′, e′, f′) whereas cells that lost their acrosomes did not display bright acrosomal fluorescence (see for instance cell c′). In these series of experiments, basal AR was 10%. Twenty-four percent of the cells underwent exocytosis when stimulated with calcium. This percentage decreased to 12% in cells pretreated with Rab3A-22A before calcium (Fig. 1, table), confirming previous observations that the chimera inhibits the AR.

Endogenous Rab3 localized to the acrosomal region in ≈50% of human sperm in the control and Rab3A-22A → calcium conditions (Fig. 1, see acrosomal staining in cells a, b, and f and quantifications in the table); the remaining cells did not exhibit specific immunofluorescence. The neck that connects the head to the tail of the sperm is a highly reactive region decorated by many antibodies and even non-immune serum (see Fig. 1*A* in Ref. 28 and 2*D* in Ref. 29) for examples); thus, staining in this domain was considered unspecific and excluded from the quantifications. The percentage of Rab3-positive cells decreased to 38% upon treatment with calcium (Fig. 1, table). Only cells that did not undergo the AR showed Rab3 immunofluorescence in the acrosomal region (cells a, b, d, and f). Cells that underwent exocytosis upon challenging with calcium (exemplified by cell c′; arrowhead points to the tip of its head, where the acrosome would have been), were not decorated by the anti-Rab3A antibodies in the acrosomal domain (cell c). These results indicate that Rab3 localizes to a compartment shed during the AR and that introduction of Rab3A-22A does not alter the acrosomal localization of sperm Rab3 assessed by fluorescence microscopy.

Rab3A-22A Blocks Exocytosis at a Stage Downstream Acrosomal Swelling—To gain insights on the mechanism that drives the inhibition caused by Rab3A-22A, we first determined its effect on acrosomal swelling. Fig. 2*A*, panel A′ shows the typical aspect of the head of a resting cell, where the acrosome is flat and even. Panel B′ illustrates a cell that underwent acrosomal swelling/deformation in response to the exocytotic stimulus (external calcium), but stopped at the docking stage because BAPTA-AM prevented intra-acrosomal calcium release (see below). The cell photographed in panel C′ was treated with Rab3A-22A before initiating the AR with calcium. Its acrosome looks like that of the cell in panel B′. Quantification of the three visually distinguishable states, intact (A′), swollen/deformed (B′, C′) and reacted (not shown but see examples in Refs. 26, 30) is plotted in Fig. 2*B*. Very few acrosomes were swollen or lost in the control condition. In contrast, external calcium elicited swelling in 30–40% of the cells preincubated with either BAPTA-AM or Rab3A-22A. There were few reacted sperm because both reagents prevent the AR. These data show that the chimeric protein does not interfere with swelling, an early stage of the exocytotic cascade. Endogenous Rab3A exchanges GDP for GTP concomitantly with swelling. In other words, Rab3A plays a positive role and the chimaera does not express its negative function during this window of time (26).

Rab3A-22A Blocks Exocytosis at a Stage Downstream Intra-acrosomal Calcium Release—The acrosome is an internal store of releasable calcium; efflux from this reservoir through inositol 1,4,5-trisphosphate (IP_3)-sensitive channels is required for the AR triggered by all inducers (reviewed in Ref. 13). Can the blocking effect of Rab3A-22A be attributed to interference with the mobilization of intracellular calcium? We used single-cell confocal microscopy in real time to answer this question. In the control condition (without any treatment), acrosomal calcium remained invariant for the length of the recording (data not shown, but see Refs. 23, 24). The AR inducer $CaCl_2$ depleted the acrosomal store, visualized with the calcium indicator Fluo3, whether or not sperm had been preincubated with Rab3A-22A (Fig. 2, *C–D*, ac, *red lines*/*bars*). Accordingly, adenophostin A, an IP_3 receptor agonist that promotes intravesicular calcium release (23) failed to rescue exocytosis halted by the chimera (Fig. 3*A*). Taken together, these results indicate that Rab3A-22A does not interfere with intra-acrosomal calcium mobilization, a relatively late stage of the exocytotic cascade.

α-SNAP and NSF Rescue the Exocytotic Block Imposed by Inhibitory Rab3As—Rab3A-22A halted the AR at a stage downstream swelling and intra-acrosomal calcium mobilization. Membrane fusion happens shortly after these events. We serendipitously found that recombinant α-SNAP reversed the exocytotic block imposed by Rab3A-22A regardless of whether

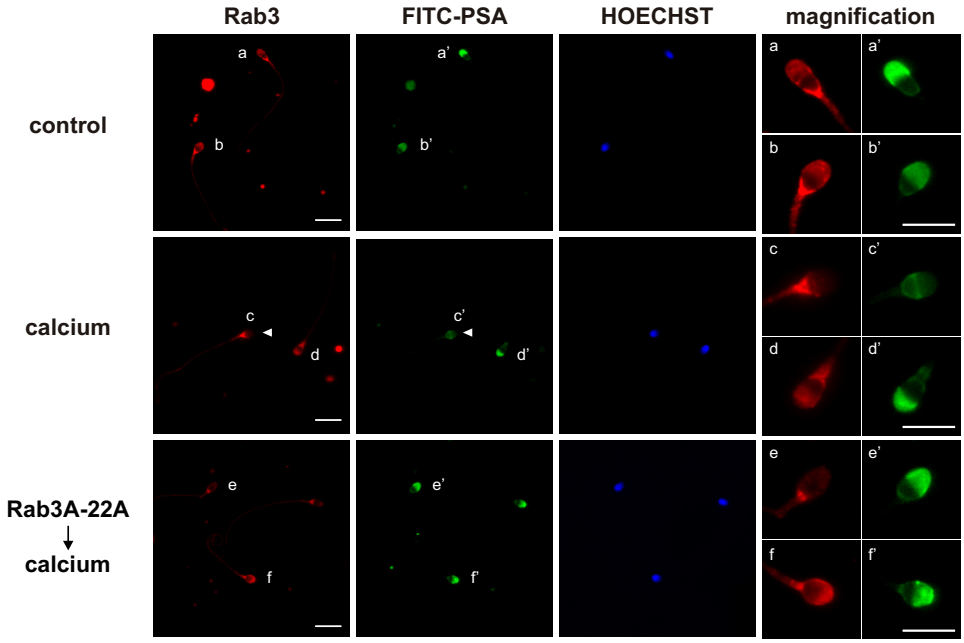

		Rab3 +	Rab3 -	% Rab3 +	FITC-PSA +	FITC-PSA -	% FITC-PSA +
control	exp 1	60	58	51	106	12	90
	exp 2	46	45	50	82	9	90
	AV			**50.5**			**90**
calcium	exp 1	37	66	36	77	26	75
	exp 2	27	40	40	51	16	76
	AV			**38**			**75.5**
Rab3A-22A → calcium	exp 1	52	60	46	97	15	87
	exp 2	41	40	49	71	10	88
	AV			**47.5**			**87.5**

**: $p < 0.01$; ***: $p < 0.001$; ns: $p > 0.05$

FIGURE 1. **Rab3A-22A does not affect the acrosomal localization of endogenous Rab3.** Capacitated, SLO-permeabilized sperm were incubated with or without 300 nM Rab3A-22A followed by 0.5 mM $CaCl_2$. Samples were incubated for 15 min at 37 °C after each addition and processed for immunofluorescence. Cells were triple stained with an anti-Rab3 antibody (*red*), FITC-PSA (to assess acrosomal status, *green*), and Hoechst 33342 (to visualize all cells in the field, *blue*). In the Rab3A-22A chimera, the amino terminus (amino acids 1–63) of Ra22A was replaced by the corresponding region of Rab3A (amino acids 1–80) (26). This portion of Rab3A does not include the peptide used to raise the anti-Rab3 antibodies. Shown are representative fields photographed after the treatments indicated on the *left*. *Control*: untreated sperm (cells **a/a'** and **b/b'** in this field are unreacted (*green*) and display acrosomal Rab3 labeling (*red*)). *Calcium*: sperm incubated with 0.5 mM $CaCl_2$. Cell **c/c'** has reacted and lacks Rab3 acrosomal staining (neither *green* nor *red*; *arrowhead* points to the tip of the head); cell **d/d'** has not reacted (*green*) and exhibits acrosomal Rab3 (*red*). Rab3A-22A→calcium shows unreacted cells (**e'** and **f'**, *green*). Cell **f** exhibits acrosomal Rab3 staining (*red*), whereas cell **e** does not. Higher magnifications of the cell heads and necks are shown on the *far right*. Scale bars: 10 μm. The actual number and percentage of cells decorated or not with anti-Rab3 antibodies and FITC-PSA in each of two independent experiments (Exp1 and Exp 2) are shown in the table. Average percentages (*AV*) of cells with acrosomal staining were compared using the Tukey's multiple comparison test; **, $p < 0.01$; ***, $p < 0.001$; *ns* indicates that statistical difference between the two groups was non-significant ($p > 0.05$).

it was added before or after initiating the AR with calcium (Figs. 3*B* and 4*A*). When added after docking in sperm loaded with the photosensitive intra-acrosomal calcium chelator NP-EGTA-AM (see Ref. 26 for a description of the experimental strategy), full-length, persistently active Rab3A behaves as the chimaera, presumably affecting exocytosis through the same mechanism. Hence, α-SNAP also reversed the exocytotic block imposed by Rab3A; and so did NSF (Fig. 3*C*). The best established role for α-SNAP in membrane fusion is to bridge NSF to *cis* SNARE complexes to disentangle them (Refs. 4, 5, 31, 32 and references therein). In several exocytotic models, these complexes are viewed as by-products of the membrane fusion reaction. Thus, we formulated the hypothesis that the inhibition caused by Rab3A and Rab3A-22A was somehow related to *cis* SNARE complexes formed after fusion pore opening. Their disassembly by α-SNAP/NSF would be required for pore dilation.

Rab3A-22A Halts Exocytosis at a Stage when Synaptobrevin-2 Is Insensitive to BoNT/B Cleavage—As shown above, α-SNAP/NSF rescued the exocytosis block imposed by Rab3A-22A and our hypothesis was that they did so by disassembling *cis* SNARE complexes. But the existence of post-fusion *cis* SNARE complexes has never been suspected in sperm: do they form after fusion pore opening during the AR? Neurotoxins (botulinum, BoNTs, and tetanus) are potent inhibitors of secretory vesicle release due to their highly specific, zinc-dependent, proteolytic cleavage of the synaptic isoforms of all SNARE proteins. SNAREs are sensitive to cleavage by neurotoxins only when not packed in tight heterotrimeric complexes (33). Whatever the steady state configuration of SNAREs might be, exocytosis in neuroendocrine cells is blocked by neurotoxins, suggesting that SNAREs go through toxin-sensitive stages (34, 35). In unstimulated sperm, on the contrary, SNAREs are stably

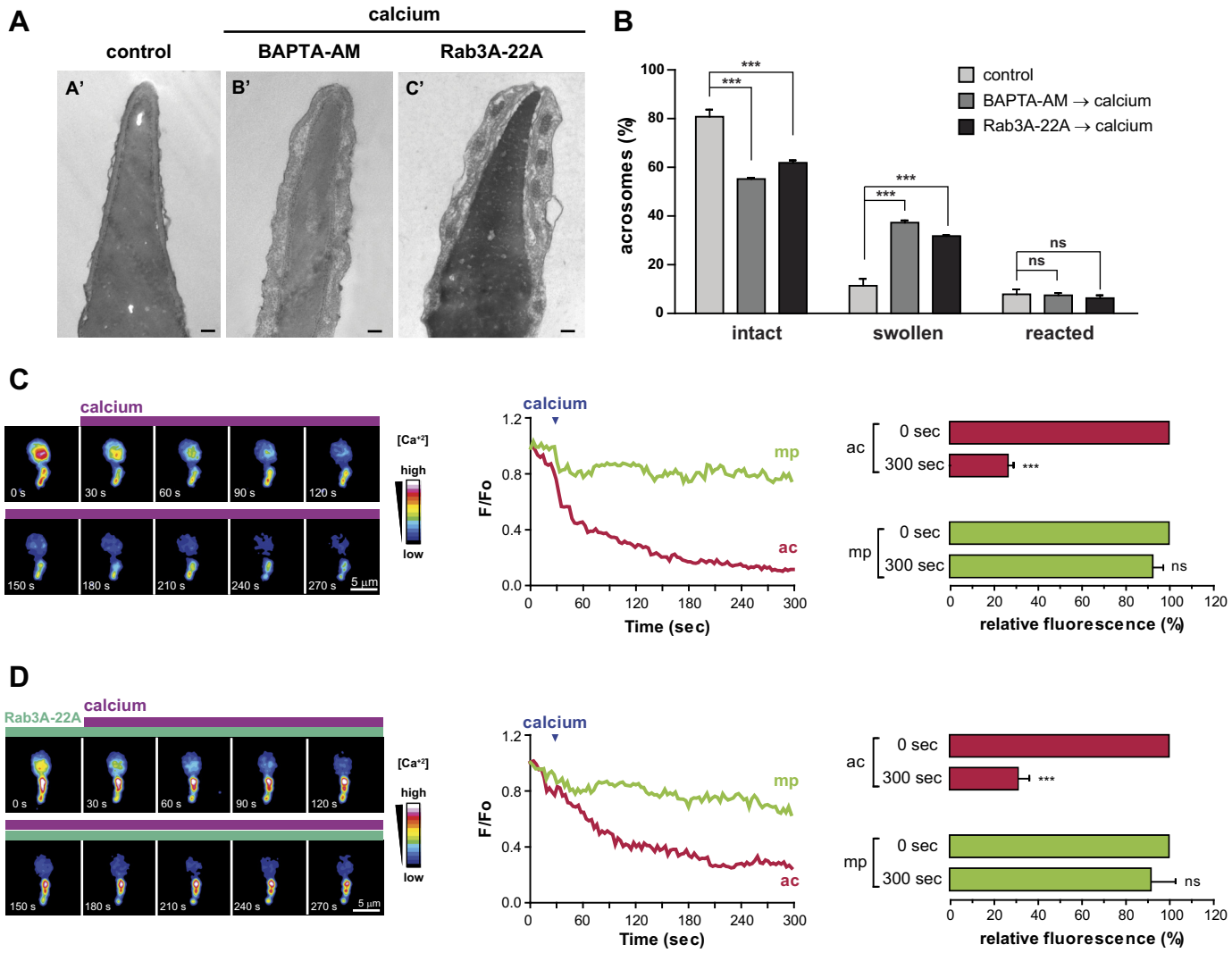

FIGURE 2. **Rab3A-22A impairs neither acrosomal swelling nor intra-acrosomal calcium release.** *A* and *B*, sperm were treated with 300 nM Rab3A-22A-GTP-γ-S and 0.5 mM $CaCl_2$ incubating for 15 min at 37 °C after each addition (*C'*). Untreated cells were the control for the morphology of unswollen, undocked acrosomes (*A'*). Cells incubated with 20 μM BAPTA-AM followed by the inducer were the control for the morphology of swollen and docked acrosomes (*B'*). *A*, electron micrographs of cells typical of each category. Size bars, 0.2 μm. *B*, quantification of the percentage of intact, swollen and reacted sperm. Data were compared using the two way Anova and the Tukey-Kramer post hoc test for two sets of data. Shown is mean ± S.E. of three independent experiments. *Asterisks* indicate significant difference (***, $p < 0.001$); *ns* indicates that statistical difference between the two groups was non-significant ($p > 0.05$). *C* and *D*, sperm were loaded with the calcium indicator Fluo3-AM (2 μM), incubated with (*D*) or without (*C*) 300 nM Rab3A-22A-GTP-γ-S and stimulated with 0.5 mM $CaCl_2$ (calcium). Fluorescence intensity was visualized, and images were processed and analyzed as in Refs. 23, 24. *Left*, images are pseudo-colored to show intensity of fluorescence. Scales are on the *right* ("warm" colors represent high $[Ca^{2+}]$). Numbers below the images indicate time in seconds. Scale bars, 5 μm. Center, each line graph shows the recording of $[Ca^{2+}]$ changes in the cell shown on the *left*. Plotted are the normalized Fluo3 fluorescence variations in the acrosome (ac, *red*) and the mid piece (mp, *green*) in response to the application of $CaCl_2$ (indicated by *vertical arrows*) *versus* time. *Right*, bar graphs illustrate the population response to each treatment (mean ± S.E.; 6–28 cells in three experiments). Shown is the relative fluorescence from the acrosomal (ac, *red*) and mid piece (mp, *green*) regions at the beginning (0 s, assigned 100%) and 270 s after the initiation of the recording. Data were evaluated with the program GraphPad Prism 5 using the Tukey-Kramer post hoc test for pairwise comparisons. *Asterisks* indicate significant difference (***, $p < 0.001$) from the initial value (single group analysis, 95% confidence interval), *ns* indicates that statistical difference from the initial value was nonsignificant ($p > 0.05$).

protected from toxin cleavage; acquisition of toxin-sensitivity is coupled to the initiation of exocytosis. When the AR begins, *cis*, toxin-resistant, SNARE complexes on the plasma and acrosomal membranes disassemble and become toxin-sensitive. SNAREs subsequently reassemble in fusion-competent *trans* complexes (13, 36). We used BoNT/B to test the hypothesis that α-SNAP/NSF rescued the Rab3A-22A block on the AR because they disassembled post-fusion *cis* SNARE complexes. This toxin is specific for synaptobrevin (37) both monomeric and engaged in partially assembled *trans* complexes (36, 38, 39); its catalytic activity is abolished by the zinc chelator TPEN. We loaded SLO-permeabilized sperm sequentially with Rab3A-22A, calcium to initiate the AR, and BoNT/B, and incubated the mixture for enough time to allow the toxin to cleave synaptobrevin; subsequently, we added TPEN to inactivate BoNT/B and α-SNAP to relieve the chimera's exocytotic block. The AR proceeded normally despite the presence of BoNT/B (Fig. 4*A*, *black bar*). Insensitivity was a consequence of introducing Rab3A-22A into sperm; otherwise, synaptobrevin was cleaved by BoNT/B and the AR, inhibited (Fig. 4*A*). In other words, when calcium stimulates the AR in the presence of Rab3A-22A, the

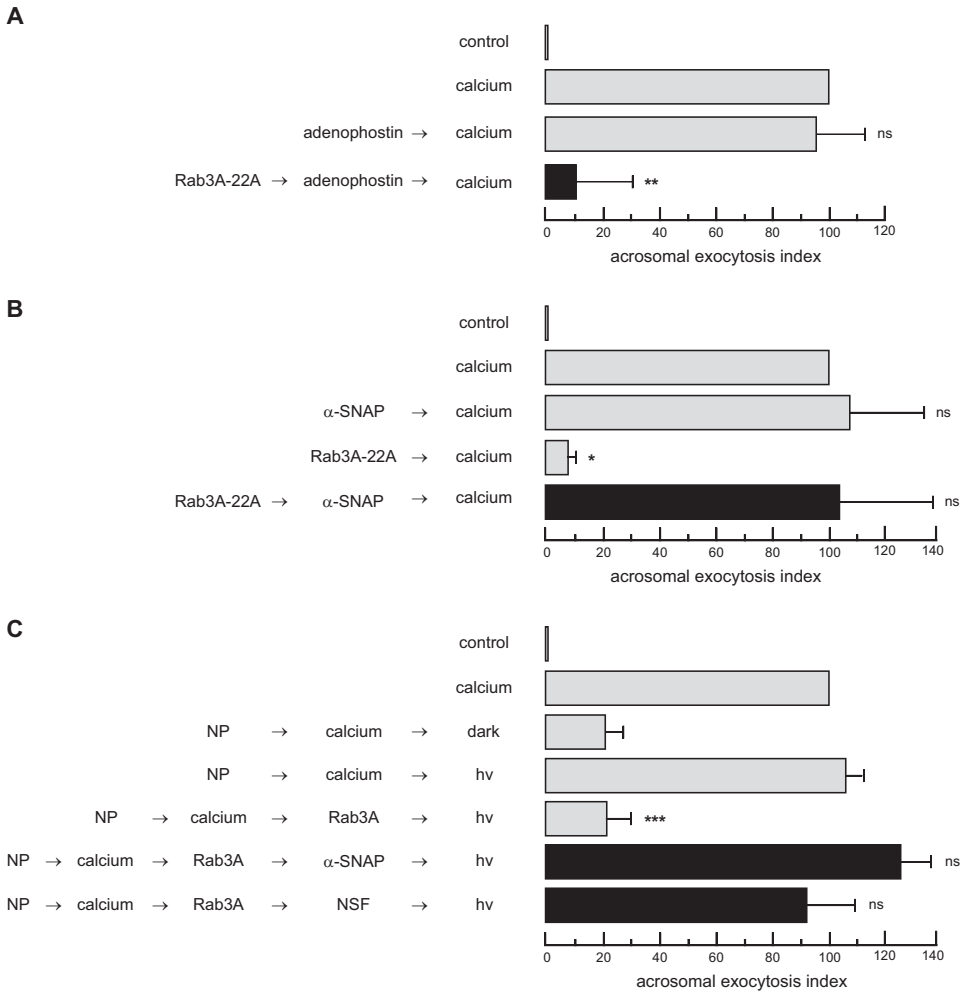

FIGURE 3. **α-SNAP/NSF rescue the exocytotic block imposed by Rab3As.** *A* and *B*, permeabilized spermatozoa were incubated with 300 nM Rab3A-22A (geranylgeranylated and loaded with GTP-γ-S). 5 μM adenophostin A (*black bar*, *A*) or 100 nM α-SNAP (*black bar*, *B*) were added to test their capacity to rescue the AR triggered by 0.5 mM $CaCl_2$ (calcium), incubating 15 min at 37 °C after each addition. *C*, permeabilized spermatozoa were loaded with 10 μM NP-EGTA-AM (NP) for 10 min at 37 °C to chelate intra-acrosomal calcium. The AR was subsequently initiated by adding 0.5 mM $CaCl_2$ (calcium). After further 15-min incubation at 37 °C to allow exocytosis to proceed up to the intra-acrosomal calcium-sensitive step, sperm were treated for 15 min at 37 °C with 300 nM Rab3A geranylgeranylated and loaded with GTP-γ-S followed by 100 nM α-SNAP or 300 nM NSF. All these procedures were carried out in the dark. UV photolysis of the chelator was induced at the end of the incubation period (hν), and samples were incubated for 5 min (*black bars*). Several controls were run in parallel (*gray bars*): background AR in the absence of any stimulation (control), AR stimulated by 0.5 mM $CaCl_2$ (calcium); lack of effect of 5 μM adenophostin A and 100 nM α-SNAP in calcium-triggered AR; inhibition of the calcium-triggered AR by the chimera; inhibitory effect of NP-EGTA-AM in the dark; the recovery upon illumination; and inhibitory effect of Rab3A (NP→calcium→Rab3A→hν). Sperm were fixed, acrosomal exocytosis was evaluated by FITC-PSA binding (indirect staining method), and data were normalized. The data represent the mean ± S.E. of three independent experiments. *A* and *B*, *, $p < 0.05$; **, $p < 0.01$, *ns*: non-significant statistical difference ($p > 0.05$) *versus* calcium; *C*, ***, $p < 0.001$, *ns*: non-significant statistical difference ($p > 0.05$) *versus* NP→calcium→hν.

exocytotic cascade advances up to a stage in which synaptobrevin is protected from BoNT/B.

We conducted the next series of experiments to test directly the configuration of synaptobrevin in sperm treated with Rab3A-22A. Monitoring SNARE proteins integrity in the presence of neurotoxins by indirect immunofluorescence is a suitable assay to determine the configuration of SNAREs in human sperm: while intact SNAREs are detected with specific antibodies, those cleaved by neurotoxins are no longer recognized (36, 40, 41). An anti-synaptobrevin-2 antibody decorated the acrosomal region in ~70% permeabilized human sperm despite pretreatment with the light chain of BoNT/B, in agreement with the notion that synaptobrevin is protected from toxin cleavage in unstimulated sperm. When the toxin was added in combination with calcium, the number of cells exhibiting synaptobrevin-2 labeling dropped significantly, indicating that the initiation of the AR had promoted the disassembly of SNARE complexes and sensitized synaptobrevin to BoNT/B (Fig. 4*B*, *top*, *gray bars*). In contrast, this SNARE remained toxin-insensitive when Rab3A-22A was also included in the assay. The only synaptobrevin-2 configuration known to be refractory to BoNT/B cleavage is the *cis* SNARE complex. If this were the case, recombinant α-SNAP (in combination with endogenous NSF) should sensitize synaptobrevin-2 to BoNT/B. This was exactly what we found (Fig. 4*B*, *black bars*). It is important to mention that SNAREs are not trapped by Rab3A-22A in the *cis* configuration typical of unstimulated sperm because the chimera inhibits the AR at a late, post-docking (26) and intra-acrosomal calcium release (Fig. 2*D*) stage. Thus, there is a second, later point during the exocytotic cascade, when SNAREs go through a BoNT/B-resistant configuration during the AR and this stage is captured by Rab3A-22A.

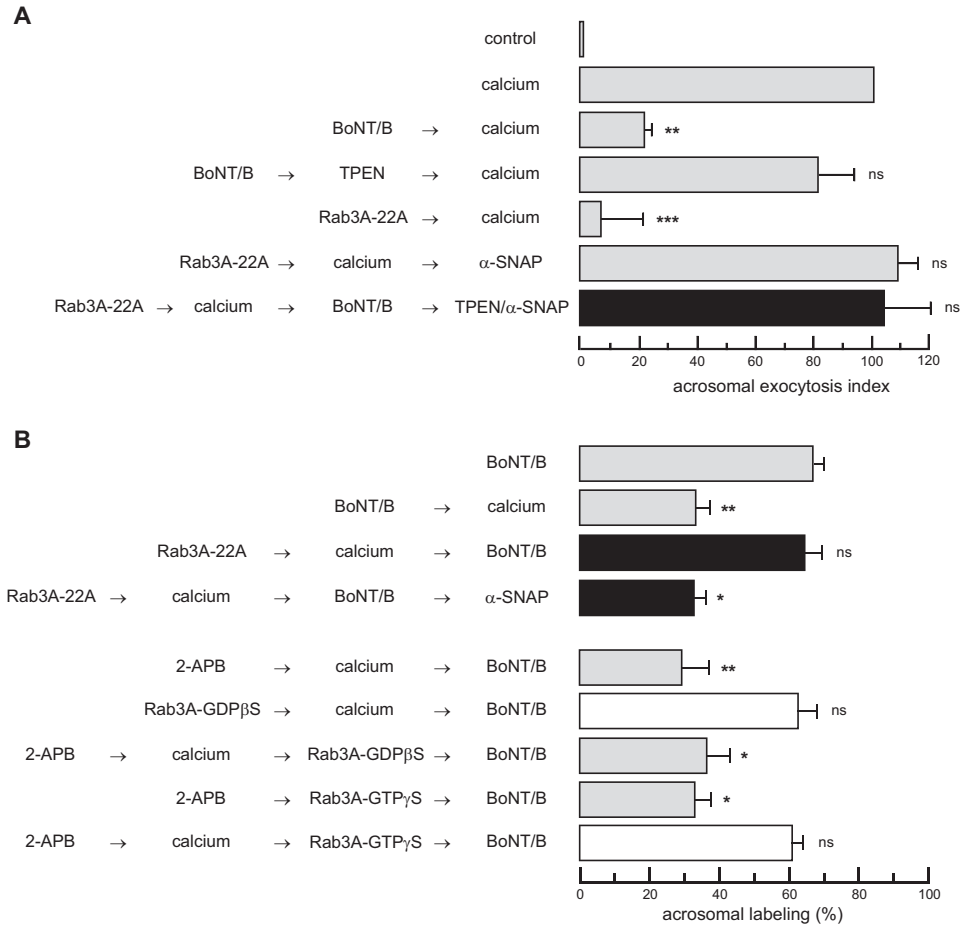

FIGURE 4. **Rab3A-22A and Rab3A-GTP-γ-S halt exocytosis at a stage when synaptobrevin-2 is insensitive to BoNT/B cleavage.** *A*, SLO-permeabilized sperm were incubated sequentially (10 min at 37 °C after each addition) with 300 nM Rab3A-22A, 0.5 mM $CaCl_2$, 100 nM light chain BoNT/B (preactivated with 5 mM DTT for 15 min a 37 °C), and 2.5 μM TPEN plus 100 nM α-SNAP (*black bar*). Several controls were run in parallel (*gray bars*): background AR in the absence of any stimulation (control), AR stimulated by 0.5 mM $CaCl_2$ (calcium); inhibition of the AR by 100 nM BoNT/B and impairing of toxin cleavage by 2.5 μM TPEN; inhibition of the AR by 300 nM Rab3A-22A and rescue by 100 nM α-SNAP. Sperm were fixed, acrosomal exocytosis was evaluated by FITC-PSA binding (indirect staining method), and data were normalized. The data represent the mean ± S.E. of three independent experiments. **, $p < 0.01$; ***, $p < 0.001$; *ns*: non-significant statistical difference ($p > 0.05$) *versus* calcium; *B*, *top,* SLO-permeabilized sperm were incubated sequentially (8 min at 37 °C after each addition) with 300 nM Rab3A-22A, 0.5 mM $CaCl_2$, 100 nM light chain BoNT/B (preactivated with 5 mM DTT for 15 min a 37 °C), and with or without 100 nM α-SNAP (*black bars*). *Bottom*, to study the effect of Rab3A's nucleotide status on the configuration of the SNARE complex, sperm were treated with 300 nM geranylgeranylated His_6-Rab3A-GDP-β-S, followed by 0.5 mM $CaCl_2$; or 100 μM 2-APB, 0.5 mM $CaCl_2$, and 300 nM geranylgeranylated His_6-Rab3A-GTP-γ-S. Finally, we added 100 nM light chain BoNT/B and incubated as before (*open bars*). Several controls were run in parallel (*gray bars*): lack of effect of 100 nM light chain BoNT/B in unstimulated sperm (BoNT/B) and synaptobrevin-2 cleavage by the toxin in cells challenged with 0.5 mM $CaCl_2$ added at the beginning or the incubation (BoNT/B→calcium) or after docking achieved by preincubating with 2-APB (2-APB→calcium→BoNT/B); synaptobrevin-2 cleavage by the toxin in cells challenged with 300 nM His_6-Rab3A-GTP-γ-S (2-APB→Rab3A-GTP-γ-S→BoNT/B); and lack of protection from toxin cleavage when GDP replaced GTP on Rab3A (2-APB→calcium→Rab3A-GDP-β-S→BoNT/B). Cells were fixed and stained with the anti-synaptobrevin-2 antibody. The data represent the mean ± S.E. of three independent experiments. *, $p < 0.05$; **, $p < 0.01$; *ns*: non-significant statistical difference ($p > 0.05$) *versus* BoNT/B.

Having established that Rab3A-22A influences the sensitivity of synaptobrevin-2 to BoNT/B, we anticipated that the GTP/GDP status of Rab3 would have consequences on the configuration of sperm SNAREs. We tested this premise by examining synaptobrevin sensitivity to BoNT/B by indirect immunofluorescence, but substituting Rab3A-22A for recombinant, full-length Rab3A loaded with either GDP-β-S or GTP-γ-S. Rab3A-GDP-β-S prevents the AR in SLO-permeabilized (26) and non-permeabilized (42) human sperm. By analogy with mutants permanently locked in the GDP-bound state, it is believed that Rab3A-GDP-β-S inhibits secretion because it sequesters the Rab3-guanine nucleotide exchange factor. If this hypothesis were correct in sperm, Rab3A-GDP-β-S would stop the exocytotic cascade at an early point, neither exogenous nor endogenous Rab3 would release GDP to bind GTP, and SNAREs would remain assembled in a *cis* configuration. This appeared to be the case, because under these conditions BoNT/B did not cleave synaptobrevin (Fig. 4*B*, *top open bar*).

Sperm incubated with persistently active, recombinant Rab3A alone, shed the acrosomal domain of their head because this protein behaves as an AR inducer. To study how Rab3A-GTP-γ-S affects steps of the cascade related to SNARE proteins, it is necessary to preserve the subcellular domain that contains them. This is accomplished with intra-acrosomal calcium chelators, that halt the AR at a stage when the acrosome is docked to the plasma membrane and SNAREs are engaged in partially assembled, BoNTs-sensitive *trans* complexes (36, 41, 43). Under these control conditions, only ≈ 25% of the sperm loaded with the calcium channel blocker 2-APB, calcium or Rab3A-GTP-γ-S and BoNT/B where decorated with the anti-

synaptobrevin-2 antibody (Fig. 4*B*). These results confirm that the two AR triggers put into motion the exocytotic cascade that disassembles the *cis* SNARE complexes pre-existent in unstimulated cells. What happens if Rab3A-GTP-γ-S is added after calcium? This is the condition in which the protein blocks the AR (Fig. 3*C*), and this is the stage when the GTPase activity of endogenous Rab3 is required. GTP hydrolysis cannot take place when the persistently active recombinant protein is present in the system (26). Interestingly, while the sequences of addition 2-APB→calcium→BoNT/B or 2-APB→Rab3A-GTP-γ-S→BoNT/B led to synaptobrevin cleavage, the sequence 2-APB→calcium→Rab3A-GTP-γ-S→BoNT/B did not (Fig. 4*B*, *bottom open bar*). This result was not a mere consequence of adding recombinant Rab3A after 2-APB and calcium because the protein loaded with GDP-β-S and added in the same sequence, did not protect synaptobrevin from BoNT/B cleavage (Fig. 4*B*, 2-APB→calcium→Rab3A-GDP-β-S→BoNT/B). To summarize, the inability of Rab3 to hydrolyze GTP freezes the AR at a late point, which is likely to correspond to an intermediate stage, transient in the absence of recombinant Rab3, when SNAREs are engaged in a post-fusion, BoNT/B-resistant, α-SNAP/NSF-sensitive (*cis*?) configuration.

Rab3A-22A Halts Exocytosis Because It Prevents Fusion Pore Expansion—If sperm SNAREs engage in *cis* complexes after membrane fusion, is the inhibition of the AR by Rab3A-22A a post-fusion event (due to interference with their disassembly)? To test this hypothesis, we adapted to SLO-permeabilized sperm a direct acrosomal staining protocol (30). In the standard (indirect staining) AR assay (used in the experiments shown in Fig. 3), the presence of the acrosomal matrix is visualized after fixation by fluorescence microscopy with the lectin PSA coupled to a fluorophore. With this method, reacted sperm are not stained and unreacted sperm exhibit fluorescent acrosomes. In the alternative (direct staining) method, fluorescent PSA is added to the culture medium from the beginning of the incubation. The acrosomes of non-reacting cells are not stained whereas those of reacting cells are. This is because PSA enters the acrosomes through the fusion pores and remains attached to the acrosomal matrix (30). Thus, the read outs of both protocols are complementary. The only condition in which acrosomes were fluorescent with both staining methods was when sperm were loaded with Rab3A-22A and challenged with calcium. Sperm incorporated the lectin through fusion pores (direct protocol, Fig. 5*A*); yet, they retained their acrosomal matrix (indirect staining, Fig. 5*B*).

Does the exocytotic cascade advance to a post-fusion (but prior to acrosomal dispersion) stage, because of Rab3A-22A inhibition? To answer this question, we applied a double staining protocol. Sperm bathed in FITC-PSA were subjected to treatment with Rab3A-22A and calcium. Cells were subsequently fixed, stained with TRITC-PSA and visualized by confocal microscopy. In the control condition, most cells were red, indicating the presence of intact acrosomes (Fig. 5*C*, *top row*). Upon treatment with calcium, ~27% of the cells underwent membrane fusion; they gained green staining because the lectin entered the acrosomal compartment through the fusion pores. These sperm were not stained red because they lost most of their acrosomal matrix (Fig. 5*C*, *asterisks*, *center row*). Approximately 21% of sperm treated with Rab3A-22A and challenged with calcium exhibited red and green acrosomes (Fig. 5*C*, bottom row shows a field enriched in double-stained cells). These findings show that fusion pores opened (green lectin entered) but the AR did not progress (red lectin stained) in sperm incubated with Rab3A-22A and calcium (see schematics in Fig. 5*D*). Because α-SNAP rescues the exocytotic block imposed by the chimera (Figs. 3*B* and 4*A*), we tested its effect in the double-staining assay. When SLO-permeabilized sperm were treated sequentially with Rab3A-22A, calcium and α-SNAP, sperm were labeled with FITC-, but not TRITC-PSA; fluorescence was undistinguishable from that in cells treated with calcium alone. We interpret these findings as indicative that α-SNAP forced fusion pore expansion, membrane vesiculation and substantial acrosomal matrix dispersal, despite the presence of Rab3A-22A in the system. Quantification of the percentage of sperm with green and orange acrosomes is depicted in Fig. 5*E*.

Several members of the fusion machinery have been implicated in fusion pore opening and dilation during exocytosis (Refs. 44–48 and references therein). The mechanisms involved, however, are far from being elucidated. Just as an example: complexin II has been claimed to induce fusion pore closure or expansion slowing (46, 49, 50), whereas complexin I appears to stimulate pore expansion (51). The novel findings reported here are: (i) sperm SNAREs engage in post-fusion, α-SNAP/NSF-sensitive complexes; (ii) their rearrangement is required to achieve vesiculation and acrosomal release; (iii) a chimeric protein containing Rab3A's amino-terminal portion, prevents these late stages by stabilizing open fusion pores. In short, as happens in many other cells, sperm fusion pores may be subjected to post-fusion regulation. It will be interesting to know if and how the mechanisms revealed by Rab3A-22A during sperm exocytosis coordinate with those operating in other cells.

Experimental Procedures

Reagents—Recombinant SLO was obtained from Dr. Bhakdi (University of Mainz, Mainz, Germany). Spermatozoa were cultured in Human Tubal Fluid media (as formulated by Irvine Scientific, Santa Ana, CA) supplemented with 0.5% bovine serum albumin (HTF medium). The mouse monoclonal anti-synaptobrevin-2 (clone 69.1, purified IgG) and rabbit polyclonal anti-Rab3 (affinity purified with the immunogen: aa 154–227 from recombinant human Rab3c; specific for all four Rab3 isoforms) antibodies were from Synaptic Systems (Göttingen, Germany). Cy™3-conjugated goat anti-rabbit as well as Cy™3-conjugated goat anti-mouse IgGs (H+L) were from Jackson ImmunoResearch (West Grove, PA). *O*-nitrophenyl EGTA-acetoxymethyl ester (NP-EGTA-AM), *N*,*N*,*N*′,*N*′-tetrakis (2-pyridymethyl) ethylenediamine (TPEN), (1,2-bis(*o*-aminophenoxy)ethane-*N*,*N*,*N*′,*N*′-tetraacetic acid)-acetoxymethyl ester (BAPTA-AM) and 1-[2-amino-5-(2,7-dichloro-6-hydroxy-3-oxo-9-xanthenyl) phenoxy]-2-(2-amino-5-methylphenoxy)ethane-*N*,*N*,*N*′,*N*′-tetraacetic acid, pentaacetoxymethyl ester (Fluo3-AM) were purchased from Life Technologies (Buenos Aires, Argentina). 2-Aminoethoxydiphenyl borate (2-APB) from Calbiochem was purchased from Merck Química Argentina S.A.I.C. (Buenos Aires, Argentina). Glutathione-Sepharose and Ni-NTA-agarose were from GE Healthcare. All other chemi-

cals were purchased from Sigma-Aldrich™ Argentina S.A., Genbiotech, or Tecnolab (Buenos Aires, Argentina).

Recombinant Proteins—Source of cDNAS, expression and purification of recombinant GST-Rab3A and GST-Rab3A-22A were as in Ref. 26. Source of cDNAS, expression and purification of recombinant light chain of botulinum toxin B (His_6-BoNT/B), His_6-α-SNAP and His_6-NSF were as in Refs. 36, 40. Source of cDNA, expression, geranylgeranylation, and loading with nucleotides of His_6-Rab3A were as described in Ref. 22.

Human Sperm Sample Preparation Procedures—Human semen samples were obtained from normal healthy donors. Semen was allowed to liquefy for 30 – 60 min at 37 °C. Following a swim-up protocol to isolate highly motile cells, sperm concentrations were adjusted to 7×10^6/ml before incubating for at

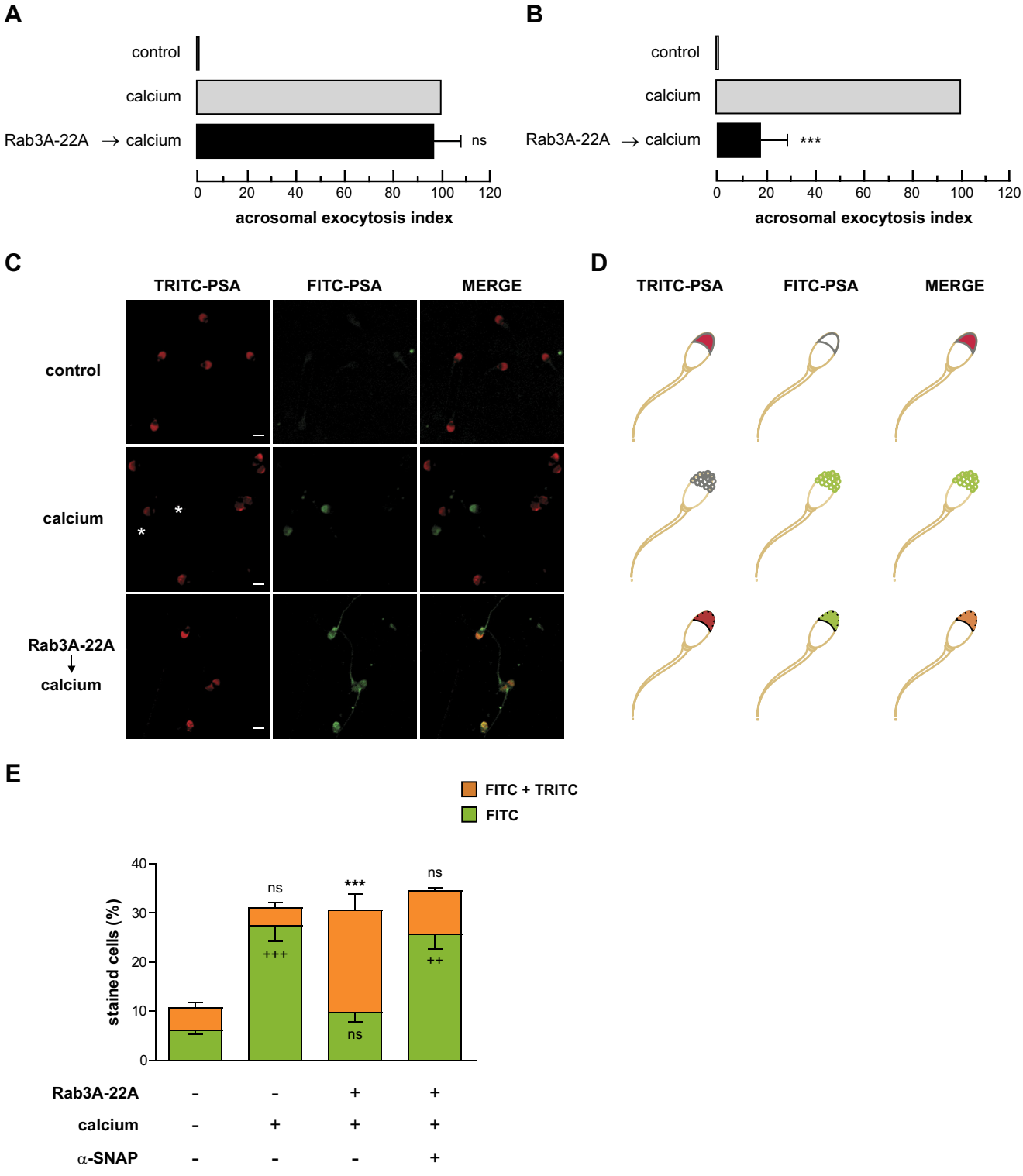

least 2 h under capacitating conditions (37 °C, 5% CO_2/95% air) in HTF. Cells were washed twice with PBS and resuspended in cold PBS containing 3 units/ml SLO for 15 min at 4 °C. Cells were washed once with PBS and resuspended in ice-cold sucrose buffer (250 mM sucrose, 0.5 mM EGTA, 20 mM Hepes-K, pH 7) containing 2 mM DTT. We added the reagents to test sequentially as indicated in the figure legends, and incubated for 8–15 min at 37 °C after each addition. Samples were processed for calcium measurements, AR assays or immunofluorescence as described later and for transmission electron microscopy as in Ref. 52. For experiments shown in Fig. 3*C*, we preloaded SLO-permeabilized sperm with photosensitive NP-EGTA-AM before incubating in the presence of calcium plus/minus recombinant proteins, carrying out all procedures in the dark. Photolysis was induced after the last incubation by exposing twice (1 min each time) to an UV transilluminator (FBTIV-614, Fisher Scientific), mixing, and incubating for 5 min at 37 °C.

Single Cell Imaging of Intra-acrosomal Calcium—Capacitated, SLO-permeabilized sperm (250 μl aliquots, 4×10^7 cells) suspended in sucrose buffer were loaded with Fluo3-AM (2 μM final concentration, dispersed with pluronic acid F-127, 0.08% final concentration) at 37 °C for 30 min. Cells were washed once to remove excess dye, resuspended in sucrose buffer and treated or not for 15 min at 37 °C with the AR blockers to test. Twenty-five μl of each sample were gently introduced into an imaging chamber fitted with a poly-L-lysine-coated 25 mm round coverslip. The chamber was transferred to the microscope stage, washed with sucrose buffer to remove unbound sperm and replenished with 300 μl fresh sucrose buffer. Cells were maintained at 37 °C at all times. After the baseline was stabilized, reagents (0.5 mM $CaCl_2$ or 300 nM Rab3A-22A followed by 0.5 mM $CaCl_2$) were added to the medium. A 473 nm laser with an emission of 535 nm was used to generate the excitation for Fluo-3. It is important to point out that the sensor only detected intracellular calcium because the AM-esterified indicator is nonfluorescent. Once the probe has diffused into a membrane-bound compartment (the acrosome in this case), esterases remove the AM moiety, trapping it. The now non-permeant Fluo3 binds calcium with high affinity and emits green-fluorescence (53, 54). A Plan Apo 60× objective was used for imaging in an Olympus FV 1000 confocal microscope. Images were collected in every 3 s using the Fluoview FV-1000 software with a total recording time of 300 s (30 s before and 270 s after addition of the inducers). Cells that came out of focus because they moved or those with uneven or no dye loading were excluded from the analysis. Fluorescence measurements in individual sperm were made by manually drawing a region of interest around the acrosome and midpiece of each cell after subtracting background noise. Results are presented as pseudo color $[Ca^{2+}]$ of 10 images collected in every 30 s. Raw intensity values were imported into Microsoft Excel and normalized using *F*/*F*o ratios after background subtraction, where *F* is fluorescence intensity at time *t* and *F*o is the baseline as calculated by averaging the 10 frames before addition of the stimuli. Cells with peak changes of $>$ 50% in F/Fo after application of $CaCl_2$ were counted as responsive. The total series of F/Fo are plotted *versus* time. Relative fluorescence (%) is the fluorescence normalized to that obtained before the addition of $CaCl_2$. Experiments were carried out three times, each repeat on a different sample. Data were plotted and analyzed with GraphPad Prism 5.

Assessment of Acrosomal Status by Post-fixation (Indirect) Staining with FITC-PSA—Sperm were spotted on teflon-printed slides, air dried, and fixed/permeabilized in ice-cold methanol for 20 s. Acrosomal status was evaluated by staining with FITC-coupled *Pisum sativum* agglutinin (FITC-PSA, 25 μg/ml in PBS) for 40 min at room temperature followed by a 20 min-wash in water (55). PSA binds α-methyl mannoside moities in proteins present in the acrosomal matrix (56). We scored at least 200 cells per condition using an upright Nikon Optiphot II microscope equipped with epifluorescence optics. Basal ("control", no stimulation) and positive ("calcium", 0.5 mM $CaCl_2$ (corresponding to 10 μM free calcium estimated by MAXCHELATOR, a series of program(s) for determining the free metal concentration in the presence of chelators; available on the World Wide Web at www.stanford.edu/~cpatton/maxc.html, Chris Patton, Stanford University, Stanford, CA)) controls were included in all experiments. Acrosomal exocytosis indices were calculated by subtracting the number of spontaneously reacted spermatozoa (basal control without stimulation, ranged from ≈5 to 25% before normalization) from all values and expressing the results as a percentage of the AR observed in the positive control (ranged from ≈15 to 60% before normalization; assigned 100% of responsive cells for normalization). We only included in our analysis results derived from experiments that produced similar responses and where the difference between basal

FIGURE 5. **Rab3A-22A halts calcium-triggered exocytosis after opening of fusion pores and prevents their expansion; α-SNAP rescues this effect.** *A*, spermatozoa were bathed in 20 μg/ml FITC-PSA, 300 nM Rab3A-22A-GTP-γ-S, and 0.5 mM $CaCl_2$ (15 min at 37 °C after each addition) and air-dried at the end of the incubations (direct staining). *B*, sperm were treated with the chimera and $CaCl_2$ as in *A*, fixed and stained with TRITC-PSA (indirect staining). The AR was scored, and data were normalized as described in Ref. 26. The data represent the mean ± S.E. of three independent experiments. ***, $p < 0.001$, *ns*: non-significant statistical difference ($p > 0.05$) *versus* calcium; *C*, capacitated, SLO-permeabilized sperm suspensions were treated as in *A*, followed or not by 100 nM α-SNAP, and double stained with FITC-PSA (direct staining) for fusion pore opening (FITC-PSA, *green*, *center*) and TRITC-PSA (indirect staining) to assess acrosomal status (TRITC-PSA, *red*, *left*). Superposition of the two fluorescence channels is depicted in the MERGE column. Shown are confocal images of representative fields (condition with α-SNAP at the end is not shown because images are identical to those in cells treated with calcium alone). Scale bars: 5 μm. Background was subtracted and brightness/contrast were adjusted to render an all-or nothing labeling pattern using Image J (freeware from NIH). *D*, schematics: control: resting, unreacted sperm. The acrosomal matrix is stained red with TRITC-PSA; membranes are not fused and therefore green lectin is excluded. Calcium: reacted sperm (corresponds to *asterisks* in *C*). FITC-PSA enters into the acrosome through the fusion pores and stains it green. Plasma and acrosomal membranes vesiculate but cannot disperse because the lectin cross-links the vesicles to the sperm head. The amount of acrosomal matrix adhered to the surface of the vesicles is insufficient to bind the red lectin. This is the same pattern as in Rab3A-22A→calcium→α-SNAP. Rab3A-22A→calcium: sperm with fused membranes. FITC-PSA enters into the acrosome through the fusion pores and stains it *green*. The chimera prevents vesiculation and dispersal of the acrosomal matrix; the latter is stained *red* by TRITC-PSA. Hence, acrosomes are *orange* in the merge image. *E*, quantification of the percentage of sperm exhibiting single or double staining. Single staining (*FITC*, *green bars*) is indicative of fused membranes and corresponds to the "calcium" pattern in *D*. Double staining (*FITC+TRITC*, *orange bars*) is indicative of fused membranes (*green*) but undispersed acrosomal matrix (*red*) and corresponds to the "Rab3A-22A→calcium" pattern in *D*. The data represent the mean ± S.E. of at least three independent experiments. ++, $p < 0.01$; +++, $p < 0.001$ *versus* FITC control; ***, $p < 0.001$ *versus* FITC+TRITC control, *ns*: non-significant statistical difference ($p > 0.05$) *versus* each control.

and stimulated conditions was of at least 8–10 percentage points. SLO-permeabilized samples with a level of spontaneously reacted sperm higher than 30% were excluded from the analysis. SLO affects neither the PSA staining pattern (compare for instance (24) for staining in non-permeabilized with (22) for staining in SLO-permeabilized human sperm) nor the number of sperm stained in the control condition (compare for instance the basal AR levels in non-permeabilized sperm, Fig. 1*A* in Ref. 57, with those in SLO-permeabilized cells, Fig. 1 in this manuscript). Data were evaluated with the program GraphPad Prism 5 using the one way Anova, Tukey's multiple comparison test. Differences were considered significant at the $p < 0.05$ level.

Indirect Immunofluorescence—We processed permeabilized human sperm as described for AR assays, adding reagents and calcium (stimulant) sequentially as indicated in the figures' keys, and incubating for 8–10 min at 37 °C after each addition before carrying on with the protocol. Sperm (5×10^5 cells) were fixed in 2% paraformaldehyde in PBS for 15 min at room temperature, centrifuged and resuspended in PBS containing 100 mM glycine to neutralize the fixative. Sperm were attached to poly-L-lysine (stock 0.1% *w*/*v* (Sigma) diluted 1:20 in water)-coated, 12 mm round coverslips by incubating for 30 min at room temperature in a moisturized chamber. Next, the plasma membrane was permeabilized with 0.1% Triton X-100 in PBS for 10 min at room temperature and washed three times with PBS containing 0.1% polyvinylpyrrolidone (PVP, average M.W. = 40,000; PBS/PVP). Nonspecific staining was blocked by incubation in 3% bovine serum albumin in PBS/PVP for 1 h at 37 °C. Anti-synaptobrevin-2 antibodies were diluted at 20 μg/ml and anti-Rab3 antibodies at 5 μg/ml in 3% bovine serum albumin in PBS/PVP, added to the coverslips, and incubated for 1 h at 37 °C in a moisturized chamber. After washing three times, 6 min each with PBS/PVP, we added Cy™3-conjugated anti-rabbit (for detection of anti-Rab3 antibodies) or anti-mouse (for detection of anti-synaptobrevin-2 antibodies) IgGs (2,5 μg/ml in 1% bovine serum albumin in PBS/PVP) and incubated for 1 h at room temperature protected from light. Coverslips were washed three times for 6 min with PBS/PVP. Cells were subsequently treated with 0.1% Triton X-100 for 15 min at room temperature, washed twice with PBS/PVP, and stained for acrosomal contents as described in "Assessment of acrosomal status by post-fixation (indirect) staining with FITC-PSA" (but without air drying), mounted with Mowiol® 4–88 in PBS containing 2 μM Hoechst 33342 and stored at room temperature in the dark until examination with an Eclipse TE2000 Nikon microscope equipped with a Plan Apo 40×/1.40 oil objective. Images were captured with a Hamamatsu digital C4742–95 camera operated with MetaMorph 6.1 software (Universal Imaging Corp.). Background was subtracted and brightness/contrast were adjusted to render an all-or nothing labeling pattern using Image J (freeware from N.I.H.). The presence of immunostaining in the acrosomal region was scored in digital images from at least 10 fields containing ≈100 cells in total. Data were evaluated with the program GraphPad Prism 5 using the one way Anova, Tukey's multiple comparison test.

Direct AR Assay/Double Staining Protocol—Capacitated, SLO-permeabilized sperm suspensions were bathed in 20 μg/ml FITC-PSA for all the incubation time. Cells were treated as described in the legend to Fig. 5, spotted on teflon-printed slides, air dried overnight and fixed/permeabilized in ice-cold methanol for 20 s, followed by a 5-min wash in water. For double staining, samples were further incubated with TRITC-PSA to assess the presence of an intact acrosomal matrix (26). Cells were recorded using an Olympus FV 1000 confocal microscope. Presence of green and/or red staining in the acrosomal region was scored by counting 100–200 cells in digital images from at least 10 fields. Data were evaluated with the program GraphPad Prism 5 using the one way Anova, Tukey's multiple comparison test. Differences were considered significant at the $p < 0.05$ level.

Author Contributions—M. F. Q., O. L., M. A. B., C. P., and P. X. D. I. performed the experiments; M. F. Q., O. L., and M. A. B. analyzed the data; C. N. T. coordinated the project and wrote the paper. All authors reviewed the results and approved the final version of the manuscript.

Acknowledgments—We thank Drs. Binz, Fasshauer, Lopez, Roggero, and Whiteheart for plasmids and Dr. Mayorga for revising this manuscript critically for important intellectual content. We also thank M. Furlán, A. Medero, E. Bocanegra, N. Domizio, J. Ibáñez, and A. Morales for excellent technical assistance.

References

1. Wu, L. G., Hamid, E., Shin, W., and Chiang, H. C. (2014) Exocytosis and endocytosis: modes, functions, and coupling mechanisms. *Annu. Rev. Physiol.* **76,** 301–331
2. Südhof, T. C. (2013) Neurotransmitter release: the last millisecond in the life of a synaptic vesicle. *Neuron.* **80,** 675–690
3. Jackson, M. B., and Chapman, E. R. (2008) The fusion pores of Ca^{2+}-triggered exocytosis. *Nat. Struct. Mol. Biol.* **15,** 684–689
4. Sorensen, J. B. (2009) Conflicting views on the membrane fusion machinery and the fusion pore. *Annu. Rev. Cell Dev. Biol.* **25,** 513–537
5. Vardjan, N., Jorgacevski, J., and Zorec, R. (2013) Fusion pores, SNAREs, and exocytosis. *Neuroscientist* **19,** 160–174
6. Chiang, H. C., Shin, W., Zhao, W. D., Hamid, E., Sheng, J., Baydyuk, M., Wen, P. J., Jin, A., Momboisse, F., and Wu, L. G. (2014) Post-fusion structural changes and their roles in exocytosis and endocytosis of dense-core vesicles. *Nat. Commun.* **5,** 3356
7. Zhao, W. D., Hamid, E., Shin, W., Wen, P. J., Krystofiak, E. S., Villarreal, S. A., Chiang, H. C., Kachar, B., and Wu, L. G. (2016) Hemi-fused structure mediates and controls fusion and fission in live cells. *Nature* **534,** 548–552
8. Buffone, M. G., Ijiri, T. W., Cao, W., Merdiushev, T., Aghajanian, H. K., and Gerton, G. L. (2012) Heads or tails? Structural events and molecular mechanisms that promote mammalian sperm acrosomal exocytosis and motility. *Mol. Reprod. Dev.* **79,** 4–18
9. La Spina, F. A., Puga Molina, L. C., Romarowski, A., Vitale, A. M., Falzone, T. L., Krapf, D., Hirohashi, N., and Buffone, M. G. (2016) Mouse sperm begin to undergo acrosomal exocytosis in the upper isthmus of the oviduct. *Dev. Biol.* **411,** 172–182
10. Sosa, C. M., Pavarotti, M. A., Zanetti, M. N., Zoppino, F. C., De Blas, G. A., and Mayorga, L. S. (2015) Kinetics of human sperm acrosomal exocytosis. *Mol. Hum. Reprod.* **21,** 244–254
11. Zanetti, N., and Mayorga, L. S. (2009) Acrosomal Swelling and Membrane Docking Are Required for Hybrid Vesicle Formation During the Human Sperm Acrosome Reaction. *Biol. Reprod.* **81,** 396–405
12. Belmonte, S. A., Mayorga, L. S., and Tomes, C. N. (2016) The Molecules of Sperm Exocytosis. *Adv. Anat. Embryol. Cell Biol.* **220,** 71–92
13. Tomes, C. N. (2015) The proteins of exocytosis: lessons from the sperm model. *Biochem. J.* **465,** 359–370
14. Barr, F. A. (2013) Review series: Rab GTPases and membrane identity: causal or inconsequential? *J. Cell Biol.* **202,** 191–199

15. Stenmark, H. (2009) Rab GTPases as coordinators of vesicle traffic. *Nat. Rev. Mol. Cell Biol.* **10,** 513–525
16. Binotti, B., Jahn, R., and Chua, J. J. (2016) Functions of Rab Proteins at Presynaptic Sites. *Cells* **5,** E7
17. Burgoyne, R. D., and Morgan, A. (2003) Secretory granule exocytosis. *Physiol. Rev.* **83,** 581–632
18. Tolmachova, T., Anders, R., Stinchcombe, J., Bossi, G., Griffiths, G. M., Huxley, C., and Seabra, M. C. (2004) A general role for Rab27a in secretory cells. *Mol. Biol. Cell* **15,** 332–344
19. Fukuda, M. (2008) Regulation of secretory vesicle traffic by Rab small GTPases. *Cell Mol. Life Sci.* **65,** 2801–2813
20. Graham, M. E., Handley, M. T., Barclay, J. W., Ciufo, L. F., Barrow, S. L., Morgan, A., and Burgoyne, R. D. (2008) A gain-of-function mutant of Munc18–1 stimulates secretory granule recruitment and exocytosis and reveals a direct interaction of Munc18–1 with Rab3. *Biochem. J.* **409,** 407–416
21. Pavlos, N. J., Grönborg, M., Riedel, D., Chua, J. J., Boyken, J., Kloepper, T. H., Urlaub, H., Rizzoli, S. O., and Jahn, R. (2010) Quantitative analysis of synaptic vesicle Rabs uncovers distinct yet overlapping roles for Rab3a and Rab27b in Ca^{2+}-triggered exocytosis. *J. Neurosci.* **30,** 13441–13453
22. Bustos, M. A., Lucchesi, O., Ruete, M. C., Mayorga, L. S., and Tomes, C. N. (2012) Rab27 and Rab3 sequentially regulate human sperm dense-core granule exocytosis. *Proc. Natl. Acad. Sci. U.S.A.* **109,** E2057–E2066
23. Ruete, M. C., Lucchesi, O., Bustos, M. A., and Tomes, C. N. (2014) Epac, Rap and Rab3 act in concert to mobilize calcium from sperm inverted question marks acrosome during exocytosis. *Cell Commun. Signal.* **12,** 43
24. Lucchesi, O., Ruete, M. C., Bustos, M. A., Quevedo, M. F., and Tomes, C. N. (2016) The signaling module cAMP/Epac/Rap1/PLCϵ/IP_3 mobilizes acrosomal calcium during sperm exocytosis. *Biochim. Biophys. Acta* **1863,** 544–561
25. Pelletán, L. E., Suhaiman, L., Vaquer, C. C., Bustos, M. A., De Blas, G. A., Vitale, N., Mayorga, L. S., and Belmonte, S. A. (2015) ADP Ribosylation Factor 6 (ARF6) Promotes Acrosomal Exocytosis by Modulating Lipid Turnover and Rab3A Activation. *J. Biol. Chem.* **290,** 9823–9841
26. Bustos, M. A., Roggero, C. M., De la Iglesia, P. X., Mayorga, L. S., and Tomes, C. N. (2014) GTP-bound Rab3A exhibits consecutive positive and negative roles during human sperm dense-core granule exocytosis. *J. Mol. Cell Biol.* **6,** 286–298
27. Yunes, R., Michaut, M., Tomes, C., and Mayorga, L. S. (2000) Rab3A triggers the acrosome reaction in permeabilized human spermatozoa. *Biol. Reprod.* **62,** 1084–1089
28. Michaut, M., De Blas, G., Tomes, C. N., Yunes, R., Fukuda, M., and Mayorga, L. S. (2001) Synaptotagmin VI participates in the acrosome reaction of human spermatozoa. *Dev. Biol.* **235,** 521–529
29. Tomes, C. N., De Blas, G. A., Michaut, M. A., Farré, E. V., Cherhitin, O., Visconti, P. E., and Mayorga, L. S. (2005) α-SNAP and NSF are required in a priming step during the human sperm acrosome reaction. *Mol Hum. Reprod.* **11,** 43–51
30. Zoppino, F. C., Halón, N. D., Bustos, M. A., Pavarotti, M. A., and Mayorga, L. S. (2012) Recording and sorting live human sperm undergoing acrosome reaction. *Fertil. Steril.* **97,** 1309–1315
31. Malsam, J., Kreye, S., and Söllner, T. H. (2008) Membrane fusion: SNAREs and regulation. *Cell Mol. Life Sci.* **65,** 2814–2832
32. Rizo, J., and Xu, J. (2015) The synaptic vesicle release machinery. *Annu. Rev. Biophys.* **44,** 339–367
33. Hayashi, T., McMahon, H., Yamasaki, S., Binz, T., Hata, Y., Südhof, T. C., and Niemann, H. (1994) Synaptic vesicle membrane fusion complex: action of clostridial neurotoxins on assembly. *EMBO J.* **13,** 5051–5061
34. Xu, T., Binz, T., Niemann, H., and Neher, E. (1998) Multiple kinetic components of exocytosis distinguished by neurotoxin sensitivity. *Nat. Neurosci.* **1,** 192–200
35. Chen, Y. A., Scales, S. J., Patel, S. M., Doung, Y. C., and Scheller, R. H. (1999) SNARE complex formation is triggered by Ca^{2+} and drives membrane fusion. *Cell* **97,** 165–174
36. De Blas, G. A., Roggero, C. M., Tomes, C. N., and Mayorga, L. S. (2005) Dynamics of SNARE assembly and disassembly during sperm acrosomal exocytosis. *PLoS. Biol.* **3,** e323
37. Pellizzari, R., Rossetto, O., Schiavo, G., and Montecucco, C. (1999) Tetanus and botulinum neurotoxins: mechanism of action and therapeutic uses. *Philos. Trans. R. Soc. Lond. B Biol. Sci.* **354,** 259–268
38. Hua, S. Y., and Charlton, M. P. (1999) Activity-dependent changes in partial VAMP complexes during neurotransmitter release. *Nat. Neurosci.* **2,** 1078–1083
39. Giraudo, C. G., Eng, W. S., Melia, T. J., and Rothman, J. E. (2006) A clamping mechanism involved in SNARE-dependent exocytosis. *Science* **313,** 676–680
40. Rodríguez, F., Bustos, M. A., Zanetti, M. N., Ruete, M. C., Mayorga, L. S., and Tomes, C. N. (2011) α-SNAP prevents docking of the acrosome during sperm exocytosis because it sequesters monomeric syntaxin. *PLoS. ONE.* **6,** e21925
41. Rodríguez, F., Zanetti, M. N., Mayorga, L. S., and Tomes, C. N. (2012) Munc18–1 Controls SNARE Protein Complex Assembly during Human Sperm Acrosomal Exocytosis. *J. Biol. Chem.* **287,** 43825–43839
42. Lopez, C. I., Belmonte, S. A., De Blas, G. A., and Mayorga, L. S. (2007) Membrane-permeant Rab3A triggers acrosomal exocytosis in living human sperm. *FASEB J.* **21,** 4121–4130
43. Bello, O. D., Zanetti, M. N., Mayorga, L. S., and Michaut, M. A. (2012) RIM, Munc13, and Rab3A interplay in acrosomal exocytosis. *Exp. Cell Res.* **318,** 478–488
44. Kesavan, J., Borisovska, M., and Bruns, D. (2007) v-SNARE actions during Ca^{2+}-triggered exocytosis. *Cell* **131,** 351–363
45. Fang, Q., and Lindau, M. (2014) How Could SNARE Proteins Open a Fusion Pore? *Physiology* **29,** 278–285
46. Neuland, K., Sharma, N., and Frick, M. (2014) Synaptotagmin-7 links fusion-activated Ca^{2+} entry and fusion pore dilation. *J. Cell Sci.* **127,** 5218–5227
47. Han, X., and Jackson, M. B. (2006) Structural transitions in the synaptic SNARE complex during Ca^{2+}-triggered exocytosis. *J. Cell Biol.* **172,** 281–293
48. Wang, X., Thiagarajan, R., Wang, Q., Tewolde, T., Rich, M. M., and Engisch, K. L. (2008) Regulation of quantal shape by Rab3A: evidence for a fusion pore-dependent mechanism. *J. Physiol.* **586,** 3949–3962
49. Archer, D. A., Graham, M. E., and Burgoyne, R. D. (2002) Complexin regulates the closure of the fusion pore during regulated vesicle exocytosis. *J. Biol. Chem.* **277,** 18249–18252
50. Dhara, M., Yarzagaray, A., Schwarz, Y., Dutta, S., Grabner, C., Moghadam, P. K., Bost, A., Schirra, C., Rettig, J., Reim, K., Brose, N., Mohrmann, R., and Bruns, D. (2014) Complexin synchronizes primed vesicle exocytosis and regulates fusion pore dynamics. *J. Cell Biol.* **204,** 1123–1140
51. Lai, Y., Diao, J., Liu, Y., Ishitsuka, Y., Su, Z., Schulten, K., Ha, T., and Shin, Y. K. (2013) Fusion pore formation and expansion induced by Ca^{2+} and synaptotagmin 1. *Proc. Natl. Acad. Sci. U.S.A.* **110,** 1333–1338
52. Pocognoni, C. A., Berberián, M. V., and Mayorga, L. S. (2015) ESCRT (Endosomal Sorting Complex Required for Transport) Machinery Is Essential for Acrosomal Exocytosis in Human Sperm. *Biol. Reprod.* **93,** 124
53. Lui, P. P., Lee, M. M., Ko, S., Lee, C. Y., and Kong, S. K. (1997) Practical considerations in acquiring biological signals from confocal microscope. II. Laser-induced rise of fluorescence and effect of agonist droplet application. *Biol. Signals* **6,** 45–51
54. Kao, J. P., Harootunian, A. T., and Tsien, R. Y. (1989) Photochemically generated cytosolic calcium pulses and their detection by fluo-3. *J. Biol. Chem.* **264,** 8179–8184
55. Mendoza, C., Carreras, A., Moos, J., and Tesarik, J. (1992) Distinction between true acrosome reaction and degenerative acrosome loss by a one-step staining method using *Pisum sativum* agglutinin. *J. Reprod. Fertil.* **95,** 755–763
56. Cross, N. L., Morales, P., Overstreet, J. W., and Hanson, F. W. (1986) Two simple methods for detecting acrosome-reacted human sperm. *Gamete Res.* **15,** 213–226
57. Branham, M. T., Bustos, M. A., De Blas, G. A., Rehmann, H., Zarelli, V. E., Treviño, C. L., Darszon, A., Mayorga, L. S., and Tomes, C. N. (2009) Epac activates the small G proteins Rap1 and Rab3A to achieve exocytosis. *J. Biol. Chem.* **284,** 24825–24839